Electronic Supplementary Material (ESI) for ChemComm.
This journal is © The Royal Society of Chemistry 2016

Supplementary Information

Selective Preparation of Elusive and Alternative Single Component Polymorphic Solid Forms Through Multi-Component Crystallisation Routes

Lynne H. Thomas, Craig Wales and Chick C. Wilson

We note that the proportions of phases present in mixed phase products was not quantified in this work; optimisation of the production routes for phase pure bulk samples was beyond the scope of this study, which instead focused on the discovery of the new templated solid forms, unambiguously characterised thorough single crystal diffraction and which are not necessarily representative of the bulk product. PXRD patterns are shown where the bulk of the sample does correspond to the new or elusive phase reported.

Section S1. Crystallisation conditions for the generation of polymorphs or molecular complexes for piroxicam, paracetamol, piracetam and the porous form of gallic acid monohydrate.

S1.1. Piroxicam (1)

Table S1.1 *Experimental conditions for co-crystallisations of piroxicam with nitrogen-heterocycles. * indicates that the form could be visually identified by the yellow colour of the crystals representing the presence of zwitterionic piroxicam within the crystal structure. Note: The formation of molecular complexes and new phases did not occur under all the conditions investigated.*

Co-Molecule	Quantity of Co-molecule	Solvent(s)	Temp(s) (°C)	Form Produced
Pyrazole	Excess (2:1 and 4:1 mass ratios)	Methanol, acetonitrile	RT, 40, 50	Form III Form II Monohydrate
3,5-dimethylpyrazole	Excess (2:1 mass ratio)	Methanol, acetonitrile	RT, 40, 50	Form III Form II Monohydrate
Pyrazine	1:1 molar, Excess (2:1 molar)	Acetonitrile	RT, 40, 50	Approx. 100% Form IV*
Indazole	1:1 molar	Methanol, acetonitrile	RT, 40, 50, 60	Form III MeOH solvate*
2,2-bipyridine	1:1 molar	Methanol, acetonitrile	RT, 40, 50	
4,4-bipyridine	1:1 molar	Methanol, acetonitrile	RT, 40, 50	
s-triazine	Excess (2:1 mass ratio)	Acetonitrile	RT, 30, 40 50	
Quinoxaline	Excess (2: 1 mass ratio)	Methanol, acetonitrile	RT, 40, 50	
1,2,3-triazole (l)	Excess (used as solvent)	N/A	RT, 60	
Pyridazine (l)	Excess (used as solvent)	N/A	RT, 40	

S1.2. Paracetamol (2)

Table S1.2 *Experimental conditions for co-crystallisations of paracetamol with nitrogen heterocycles. All crystallisations were carried out in a 1:1 molar ratio. The quantities of each polymorph present were evaluated through quantitative phase analysis of powder diffraction patterns using the program PolySNAP.*[1]

Co-molecule	Solvent	Form produced	Comment
Pyrazole	Methanol	Form I	RT or 40°C
	Methanol	100% Form II	50°
	Acetone	Form I	RT or 50°C
3,5-dimethylpyrazole	Methanol	Mixture	50°C
	Acetone	Mixture	
Pyrazine	Methanol	Form I	RT or 40°C
	Methanol	100% Form II	50°C
	Acetone	Form I	50°C

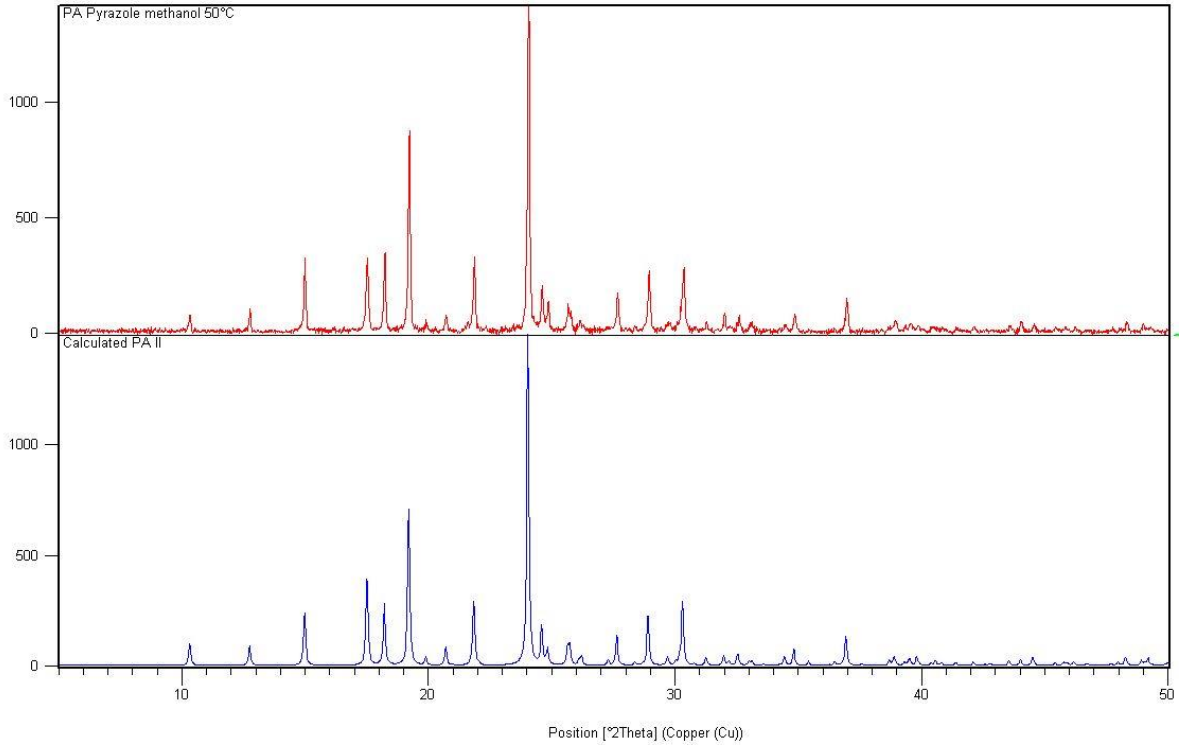

Figure S1.2.1. PXRD of the co-crystallisation of paracetamol with pyrazole in methanol at 50°C (top, red). The pattern shows PA II in 100% yield (calculated PA II shown below in blue). The pattern indicates no pyrazole is present.

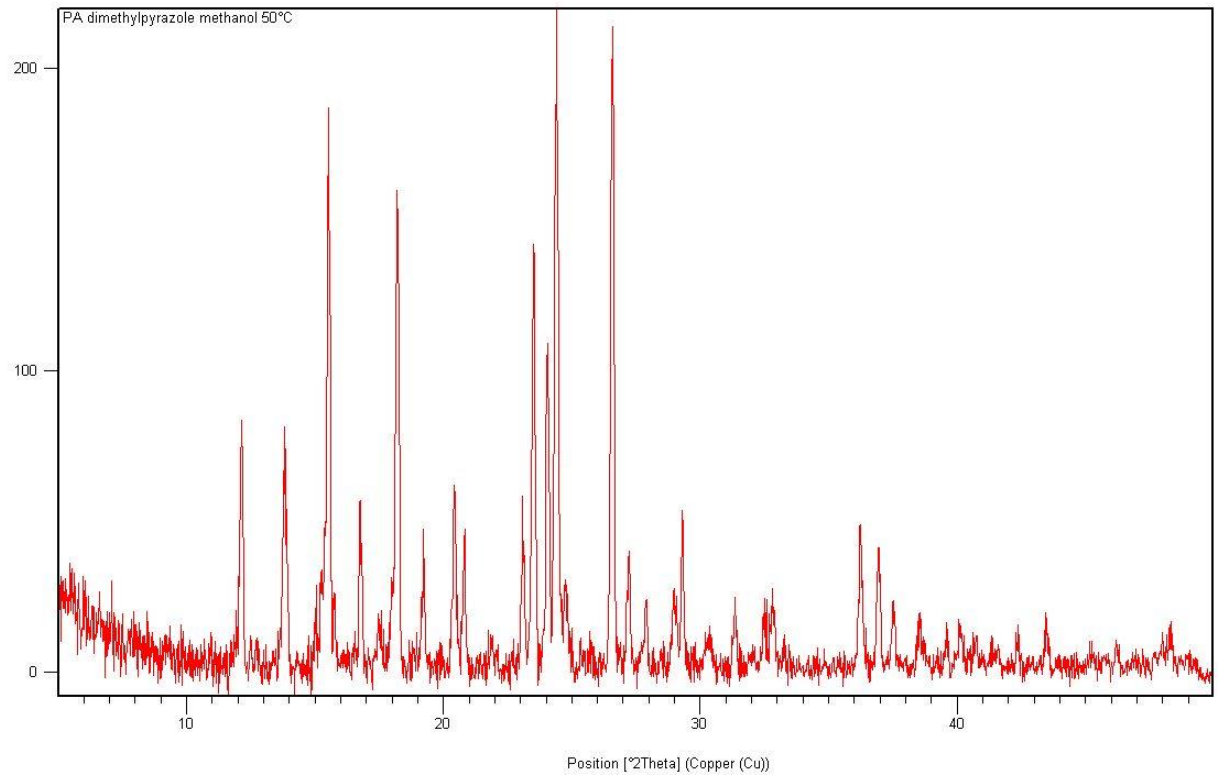

Figure S1.2.2. PXRD of the co-crystallisation of paracetamol with 3,5-dimethylpyrazole in methanol at 50°C. The pattern shows a mixture of PA I and PA II with only small quantities of 3,5-dimethylpyrazole detected.

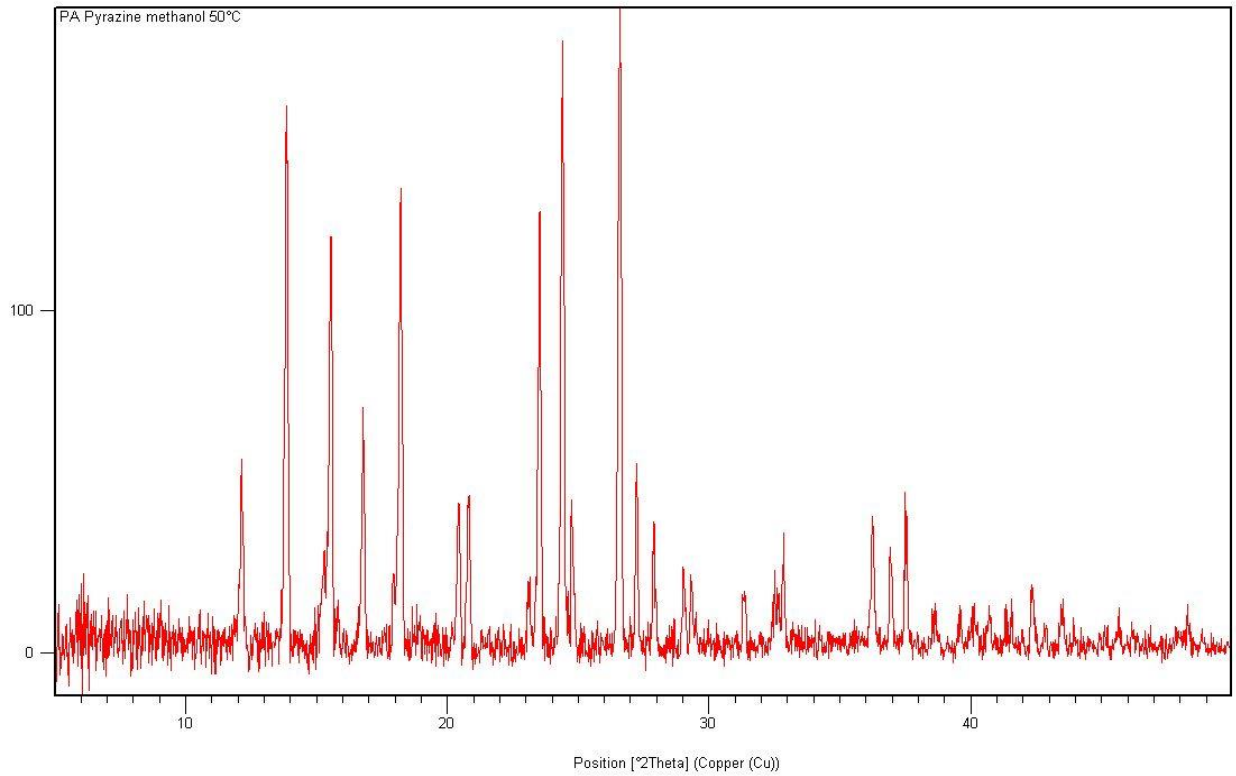

Figure S.1.2.3. PXRD of the co-crystallisation of paracetamol with pyrazine in methanol at 50°C. The pattern shows PA II in 100% yield. The majority of the pyrazine appears to have sublimed during the evaporation process.

S1.3. Piracetam (3)

Table S1.3 *Experimental conditions for co-crystallisations of piracetam with nitrogen-heterocycles. All crystallisations resulted in a mixture of piracetam form I and the more stable form II.*

Co-Molecule	Quantity of Co-molecule	Solvent(s)	Temp(s) (°C)
Pyrazole	Excess (2:1 mass ratio)	MeOH	50
None	None	MeOH	50

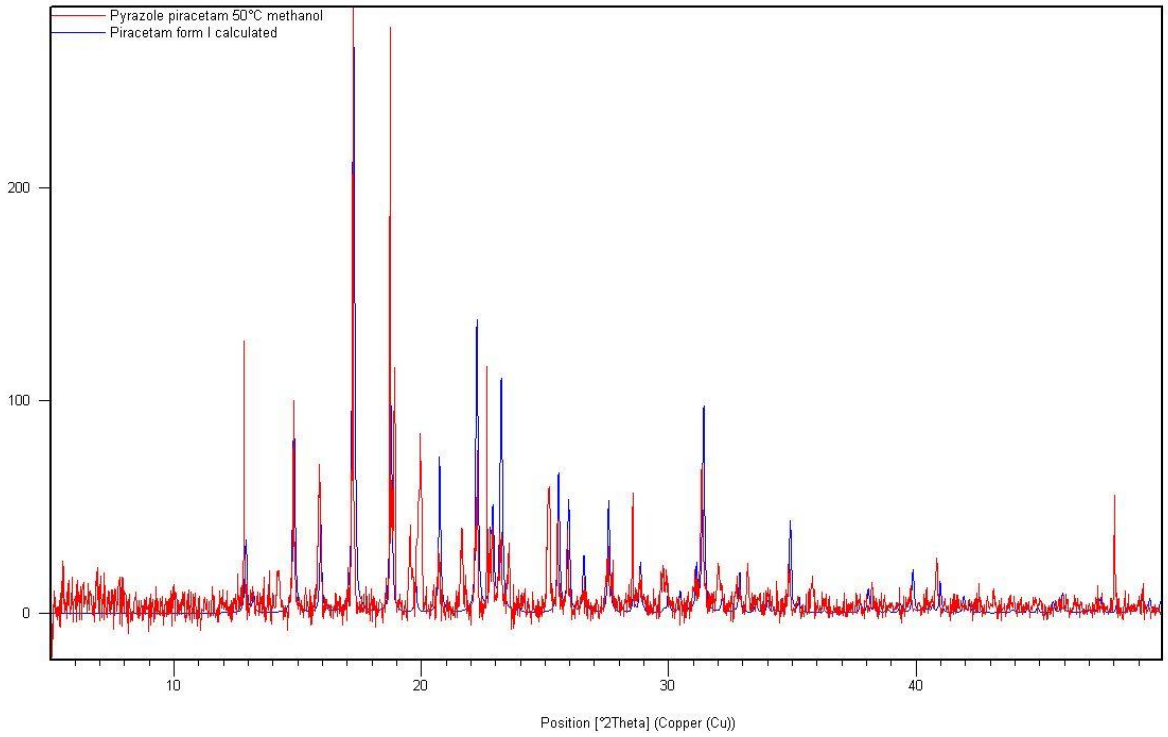

Figure S1.3.1. PXRD of the co-crystallisation of piracetam with pyrazole (1:2 mass ratio) in methanol at 50°C (red). The pattern shows a mixture of piracetam form I (blue) and form II (remaining peaks).

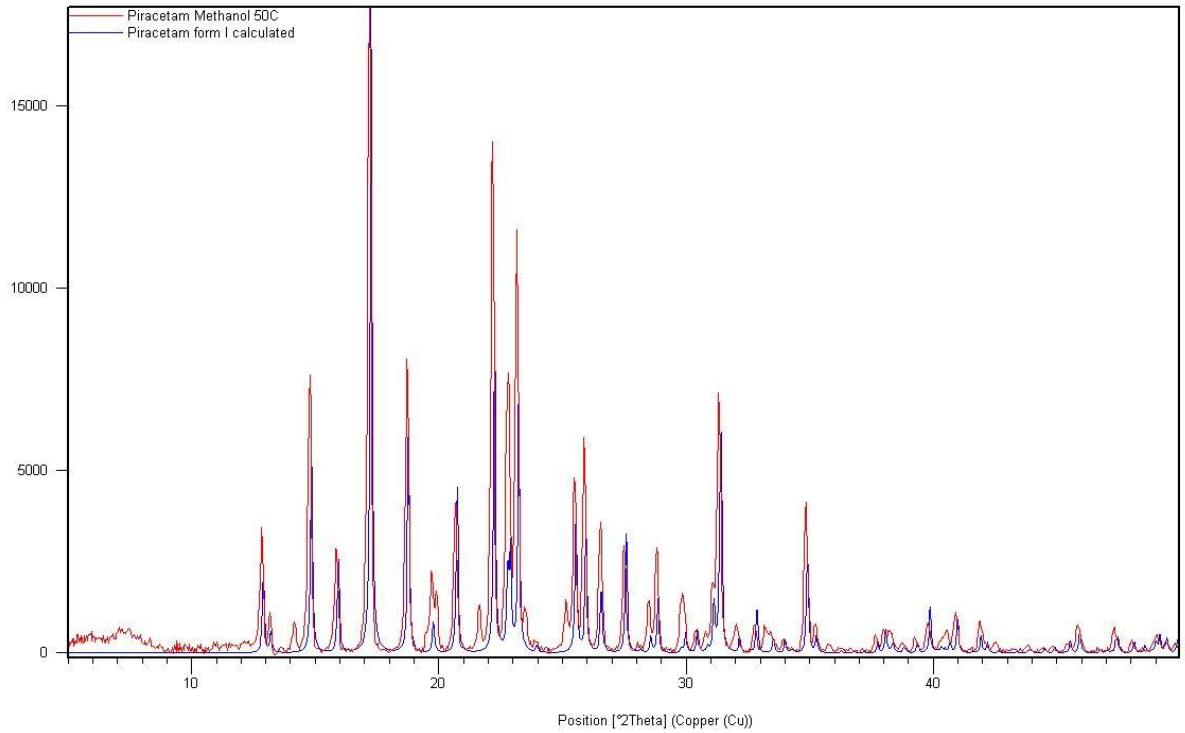

Figure S1.3.2. PXRD of the recrystallisation of piracetam in methanol at 50°C (red). The pattern shows a mixture of piracetam form I (blue) and form II (remaining peaks).

S1.4 Gallic Acid Monohydrate (4.H_2O)

Table S1.4. *Experimental conditions for co-crystallisations of gallic acid with piracetam to generate a new porous form of gallic acid monohydrate. *crystallisation from ethyl acetate led to the formation of a molecular complex between piracetam and gallic acid.*

Co-Molecule	Quantity of Co-molecule	Solvent(s)	Temp(s) (°C)
Piracetam	1:1 molar ratios	methanol, ethanol, acetone or acetonitrile*	RT

Section S2. New Solid Forms of Piroxicam (1)

S2.1. Piroxicam Form III (1-III)

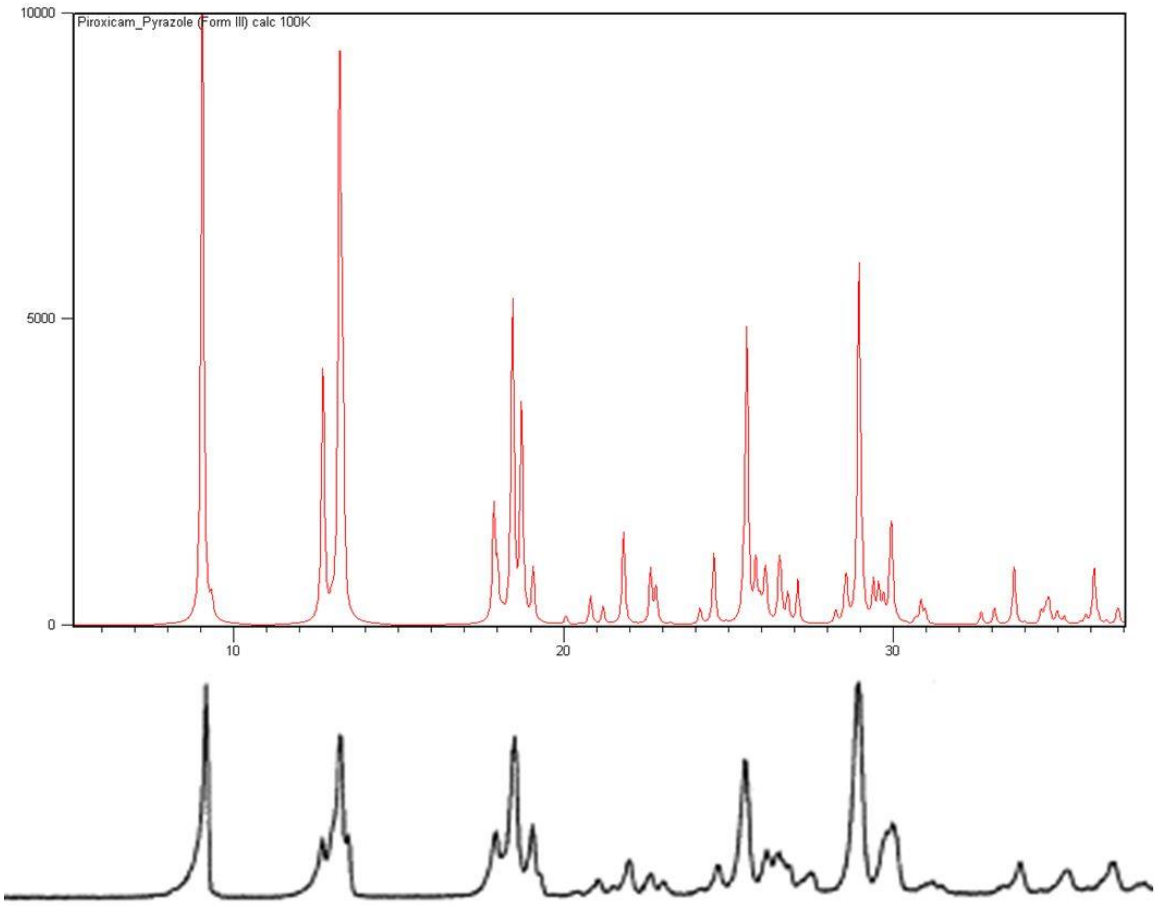

Figure S2.1.1. *The calculated PXRD pattern for piroxicam form III (top; calculated from the single crystal structure obtained here) and the experimental PXRD pattern from a previous study[1] (bottom).*

Single crystal X-ray diffraction data for this complex were collected on a Bruker AXS Apex II CCD diffractometer at 100K. Single crystals were grown via solvent evaporation at 50°C using pyrazole as the co-molecule and acetonitrile as the solvent. Form II and the monohydrate were also found within the vial.

The crystal structure of PX form III consists of a single molecule in the asymmetric unit which forms the same PX dimers that are found in PX form I.[2] These dimers are formed via N-H···O hydrogen bonds between the amide N-H and the sulfonyl oxygen atoms (Figure S2.1.2). The N-H···O hydrogen bond length in this dimer is similar to that found in form I, although a slightly longer donor-acceptor distance is observed despite the structure being determined at lower temperature (100K c.f. 300K for form I) (Table S2.1.1). The structure of form III is also layered in a similar fashion to form I (Figure S2.1.3a), with the methyl and sulfonyl groups bridging between the layers. The differences between

form I and form III are seen in the extended packing and the weaker hydrogen bonds. PX molecules in form III link to PX molecules above, via C-H···O hydrogen bonds between the pyridine aromatic C-H groups and the second sulfonyl oxygen atom (Figure S2.1.3b). The second sulfonyl oxygen in PX I forms hydrogen bonds to the benzene C-H group of a PX molecule above (Figure S2.1.3c), resulting in very different relative positions of PX molecules in different layers (Figure S2.1.3d).

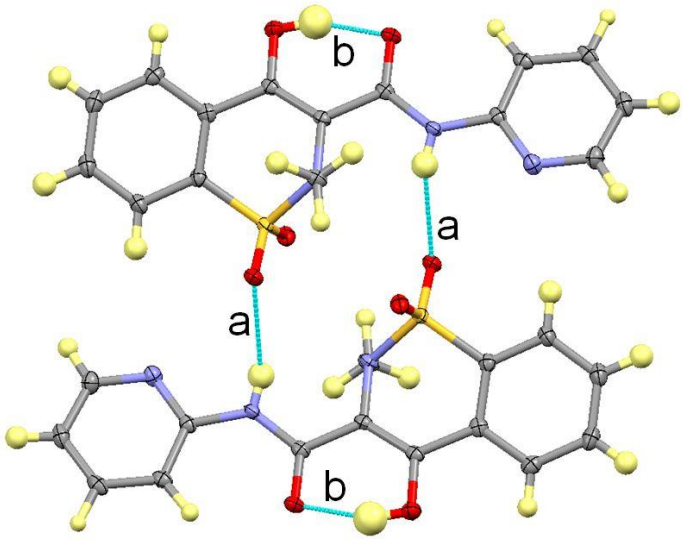

Figure S2.1.2. *The hydrogen bonded PX dimers formed in piroxicam form III.*

Table S2.1.1 *Hydrogen bond distances and angles in the piroxicam dimers in PX form I*[3] *and form III (refer to Figure S2.1.2 for key).*

Polymorph	Temp (K)	H-Bond	D-H (Å)	H···A (Å)	D···A (Å)	∠D-H···A (°)
III	100	a	0.80(2)	2.41(2)	3.059(2)	139(2)
		b	0.89(3)	1.70(3)	2.544(2)	157(2)
I[3]	300	a	0.84(3)	2.44(3)	3.053(3)	130(3)
		b	0.81(3)	1.79(3)	2.561(3)	156(4)

A second C-H group of the pyridine ring forms C-H···O hydrogen bonds with the hydroxyl oxygen of a PX molecule below (C···O = 3.384(2) Å) (Figure S2.1.4). Molecules above and below each other are further linked by weak hydrogen bonds between the methyl C-H groups and the amide carbonyl oxygen (C···O = 3.363(2) Å) as well as well as π···π interactions between the amide carbonyl double bonds, with approximately 3.049 Å between the centroids of the π bonds (Figure S2.1.5).

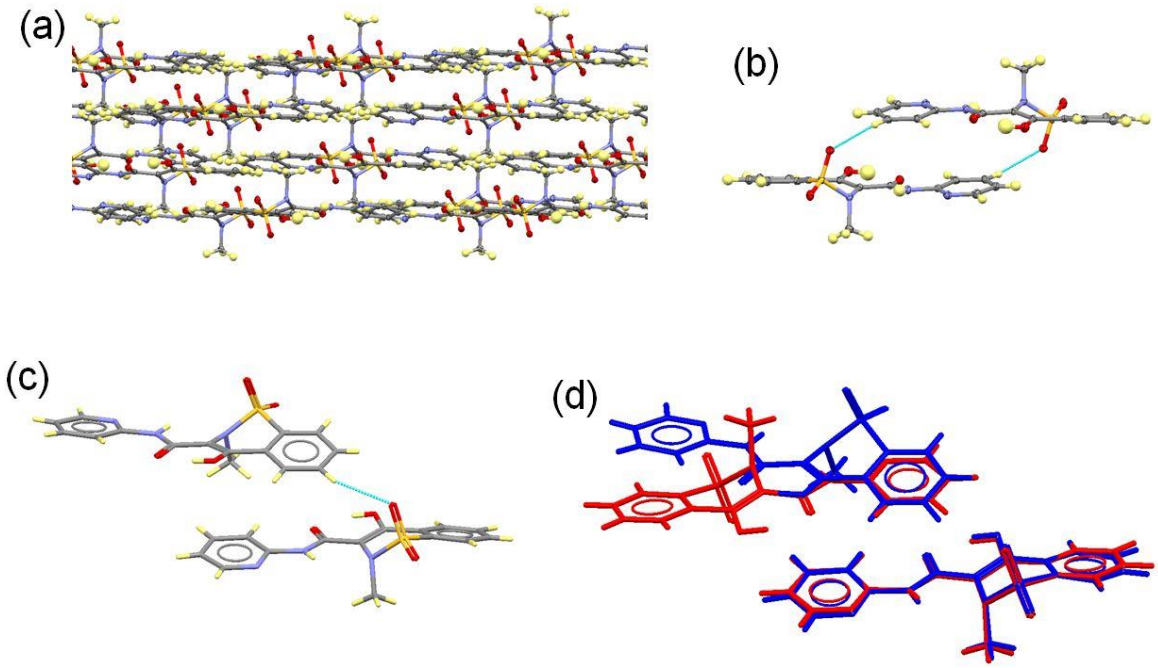

Figure S2.1.3. *Crystal packing in piroxicam form III. (a) The layered arrangement of molecules. (b) C-H···O hydrogen bonds between a pyridine C-H and the sulfonyl O of PX molecules above and below each other. (c) The similar C-H···O hydrogen bonds in PX form I, where the sulfonyl oxygen instead forms hydrogen bonds with the benzene C-H of the PX molecule above. (d) An overlay of the crystal structures of PX I and III, showing the difference in the relative arrangement of the PX molecules above each other.*

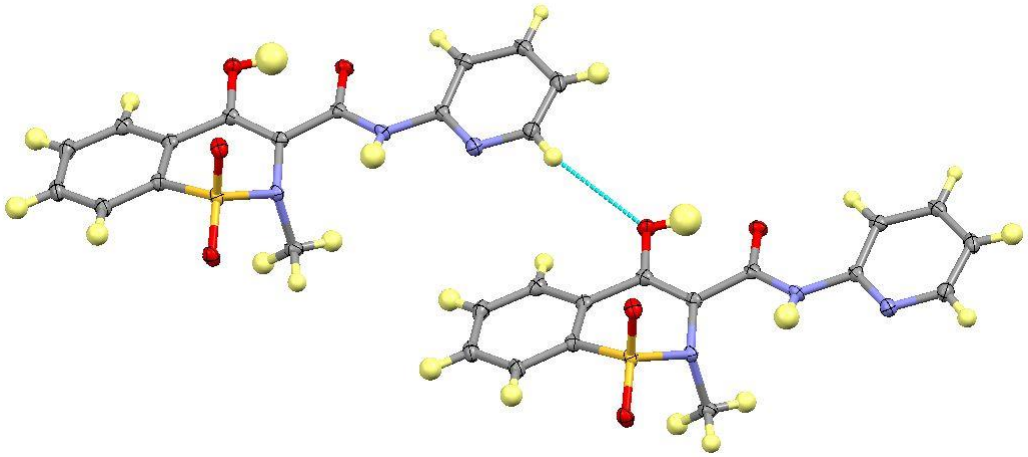

Figure S2.1.4. *C-H···O interactions between a pyridine C-H group and the hydroxyl oxygen in piroxicam form III.*

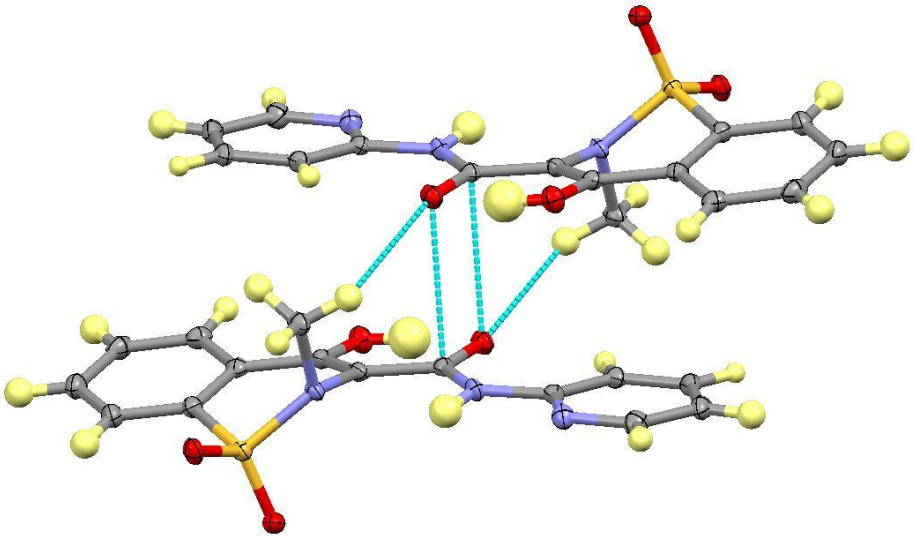

Figure S2.1.5. *C-H···O and π···π interactions involving the amide oxygen in piroxicam form III.*

S2.2. Piroxicam Form IV (1-IV) – A mixed ionisation state polymorph

Single crystals of form IV were grown by solvent evaporation at 50°C using pyrazine as the co-component (1:2 mass ratio) and acetonitrile as the solvent. Crystals of form IV could easily be identified in the crystallization vial by their needle shape and yellow colouring reflecting the presence of piracetam molecules in the zwitterionic form. Occasionally a molecular complex with pyrazine could be identified along with forms I, II or the monohydrate within the same crystallization vial. Single crystal X-ray diffraction data were collected on a Rigaku R-AXIS RAPID Image Plate diffractometer at 100K. Single crystals were small and of poor quality and did not diffract well. Several attempts at data collection were carried out, including data collection at the I19 beamline at Diamond; the data presented is the best which could be obtained from the poor quality crystals.

Anisotropic refinement caused the thermal parameters of one carbon atom (C75) to become abnormally elongated along one axis; its thermal parameters were therefore fixed as isotropic to obtain a plausible approximation. This is likely due to the presence of a small amount of orientational disorder of this molecule (<10%); two positions for the sulfonyl group could be identified but significant overlap for the remainder of the molecule meant that it was not possible to fully resolve two positions. A model with a single position was therefore adopted in the final model. Modelling of this disorder was further hindered by the fact that the data were weak and of poor resolution with a high R_{int} (0.106), meaning that a model with a single position for this molecule was therefore adopted in the final model. Additionally, H-atoms could not be accurately located using the Fourier difference synthesis. All hydrogen atoms were therefore placed on calculated positions and refined as riding on

the atoms to which they were bonded. The piroxicam tautomer present was inferred by the conformation of the molecules and the hydrogen bonding interactions. The yellow colour of the crystals further evidenced the presence of the zwitterionic tautomer.

Piroxicam form IV features five molecules in the asymmetric unit and is unusual in that four of the molecules are present as the non-ionised tautomer (PXN) and the other as the zwitterionic tautomer (PXZ). In addition to the different distribution of hydrogen atoms within the tautomers, there is a substantial conformational difference between the neutral and zwitterionic forms, offering unambiguous conclusions to be drawn regarding the tautomers present from the X-ray data. The PXN molecules dimerise with non-equivalent PXN molecules through two N-H···N hydrogen bonds (Figure S2.2.1), with two symmetry independent dimers formed in this way. The hydrogen bonding in this dimer is unique from that seen in any of the other three polymorphs of PX. The N-H···N hydrogen bonds in one dimer are slightly stronger than in the other, with the PXN molecules in the weaker dimer possessing stronger intramolecular O-H···O hydrogen bonds (Table S2.2.1).

Equivalent PXZ molecules also dimerise, although the presence of the different tautomer results in a completely different type of dimer to that formed by the PXN molecules. The dimer is formed by two moderately strong charge-assisted bifurcated DHAA N^{+}-H···O hydrogen bonds between the protonated pyridinal nitrogen and the amide carbonyl oxygen (Figure S2.2.1). This type of dimer is formed by PXZ molecules in all previously reported complexes containing PXZ.[3,4]

The PXZ dimers are linked to PXN molecules through a number of weak CH···O hydrogen bonds (Figure S2.2.2). Pyridine C-H groups of PXN molecules form charge assisted hydrogen bonds to the enolate oxygen of the PXZ molecules (C···O = 3.440 (7)Å) (Figure S2.2.2a). Benzene and pyridine C-H groups of PXZ molecules also form hydrogen bonds to the sulfonyl oxygen atoms of PXN molecules (C···O = 3.445(7) Å and 3.398(9) Å respectively) (also Figure S2.2.2a). Similar hydrogen bonds are formed from the benzene and pyridine C-H groups of PXN molecules to the sulfonyl oxygen atoms of PXZ molecules (C···O = 3.480(8) Å and 3.264(8) Å) (Figure S2.2.2b).

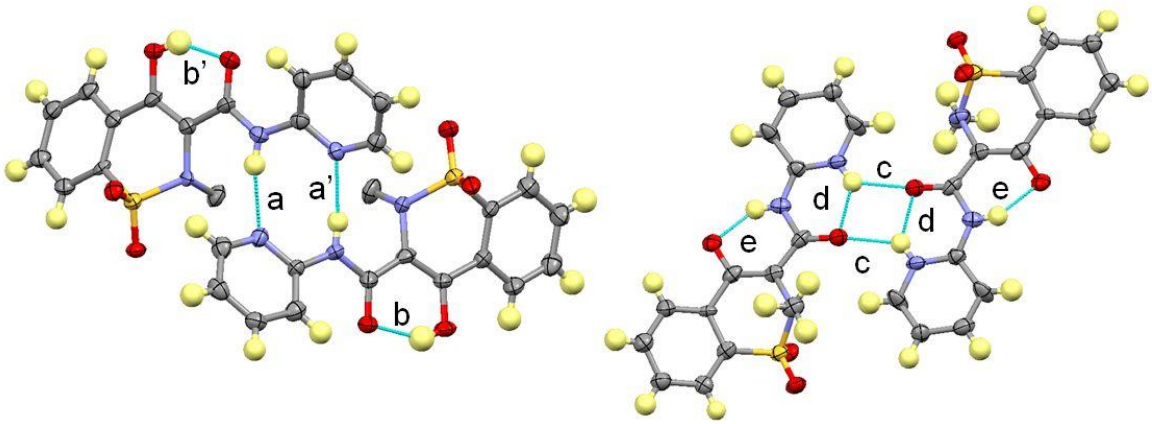

Figure S2.2.1. *The dimers formed in piroxicam form IV. Non-ionised molecules dimerise through N-H···N hydrogen bonds (LHS - methyl hydrogen atoms omitted), whilst the zwitterionic molecules dimerise via charge-assisted bifurcated DHAA N^{+}- H···O hydrogen bonds (RHS).*

Table S2.2.1. *Hydrogen bond distances and angles in piroxicam form IV (refer to Figure S2.2.1 for key). Note that the numbers 1 and 2 refer to the symmetry independent dimers of PXN molecules. Hydrogen atoms were placed on calculated positions due to the poor quality of the data.*

H-Bond	D-H (Å)	H···A (Å)	D···A (Å)	∠D-H···A (°)
a1	0.86	2.16	2.934(7)	149
a1’	0.86	2.14	2.933(8)	153
a2	0.86	2.18	2.985(7)	155
a2’	0.86	2.14	2.953(7)	158
b1	0.82	1.79	2.518(7)	148
b1’	0.82	1.81	2.531(6)	146
b2	0.82	1.78	2.509(8)	148
b2’	0.82	1.77	2.498(6)	147
c	0.86	2.25	2.930(7)	136
d	0.86	1.99	2.638(7)	131
e	0.86	1.80	2.533(7)	141

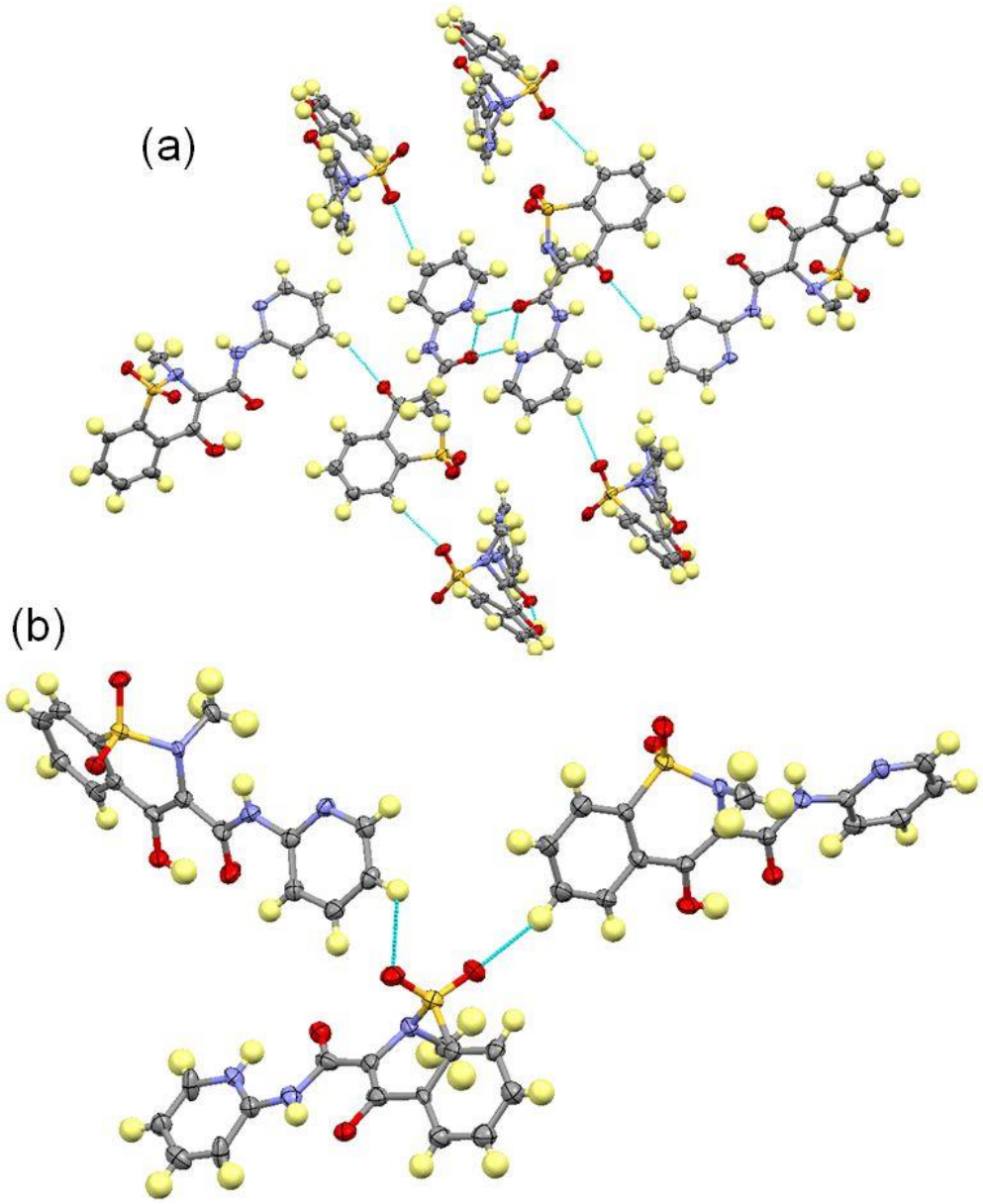

Figure S2.2.2. *Weak C-H···O hydrogen bonds linking PXZ dimers to PXN molecules in piroxicam form IV. (a) C-H···O hydrogen bonds from the PXZ pyridine and benzene ring CH groups to the PXN sulfonyl oxygen atoms and from the PXN pyridine ring C-H group to the PXZ enolate oxygen. (b) C-H···O hydrogen bonds involving the PXZ sulfonyl oxygen atoms.*

The pairs of PXN molecules in both of the symmetry independent PXN dimers do not lie co-planar and these dimers are linked to each other through further moderate to weak strength C-H···O hydrogen bonds (Figure S2.2.3) between benzene C-H groups and sulfonyl oxygen atoms (C···O = 3.079(9) Å, 3.218(9) and 3.112(9) Å). The staggered nature of the dimers results in a non-layered structure unlike PX I and PX II. Further C-H···O hydrogen bonds between PXN molecules are present involving the methyl group and hydroxyl oxygen groups (C···O = 3.266(7) Å) and π···π interactions are

also present between benzene rings, with approximately 3.309 Å between the planes of the rings (Figure S2.2.4)

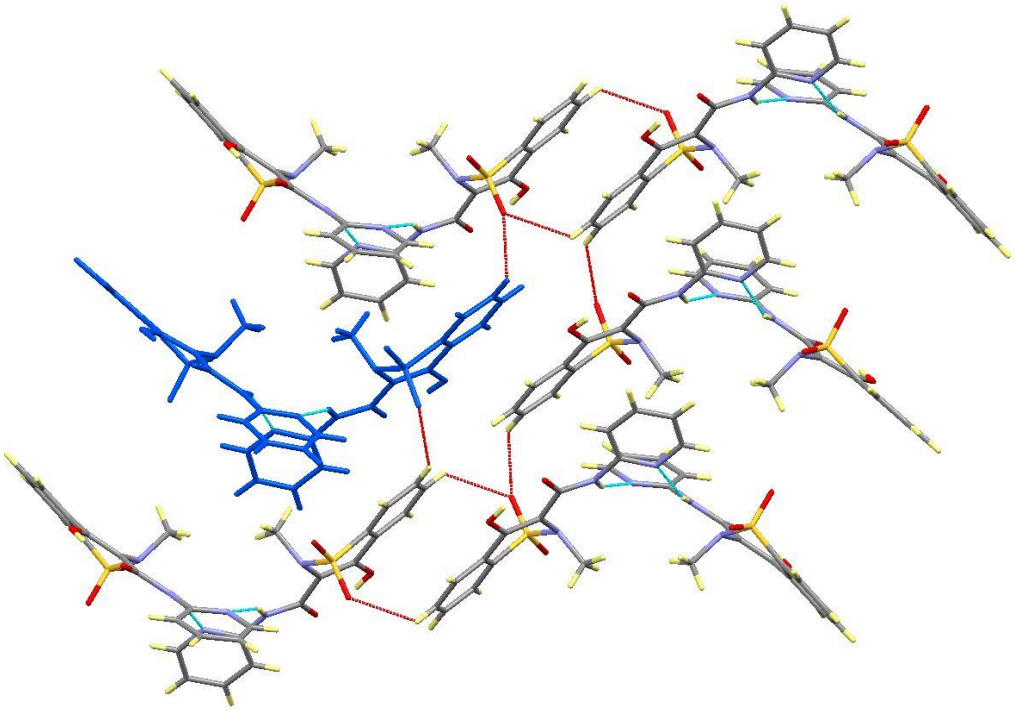

Figure S2.2.3. *Weak C-H···O hydrogen bonds (red dashed lines) linking PXN dimers in piroxicam form III. The diagram also shows the staggered nature of the PXN dimers (one dimer highlighted in blue).*

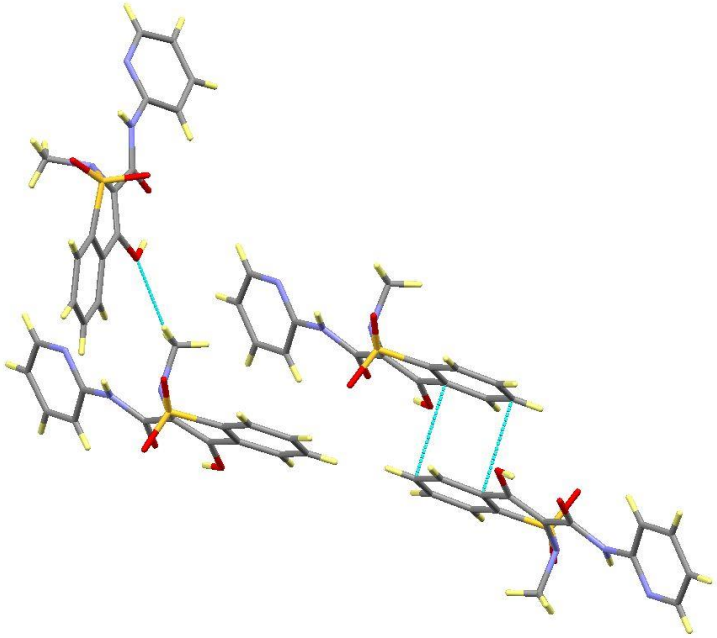

Figure S2.2.4. *Further weak interactions between PXN molecules showing the C-H···O hydrogen bond between the methyl and hydroxyl groups and π···π interactions between the benzene rings.*

S2.3. Piroxicam MeOH solvate (3:1) (1-MeOH)

Single crystals were grown using solvent evaporation at 60°C using indazole as the co-component and methanol as the solvent. Piroxicam form I was found to crystallise concomitantly but the

methanol solvate crystals could be easily identified in the vial by their yellow colouring reflecting the presence of the zwitterionic form of piroxicam. Single crystal X-ray diffraction data were collected on a Rigaku R-AXIS RAPID Image Plate diffractometer at 100K. Single crystals were small and of extremely poor quality and did not diffract well. Several attempts at data collection were carried out, including data collection at the I19 beamline at Diamond; the data presented is the best which could be obtained from the poor quality crystals.

Anisotropic refinement of the heavy atoms resulted in implausible thermal parameters of a number of atoms. Heavy atoms were therefore refined isotropically in the final refinement cycles. To locate the hydroxyl hydrogen (H44) of the methanol molecule, anisotropic refinement of the heavy atoms was first carried out. H44 was then located and the O-H distance constrained to 0.9Å and the thermal parameter refined as riding on the oxygen to which it is bonded. All other hydrogen atoms were then placed on calculated positions and refined as riding on the atoms to which they were bonded. The piroxicam tautomer present was inferred by the conformation of the molecules and the hydrogen bonding interactions. The yellow colour of the crystals further evidenced the presence of the zwitterionic tautomer.

Crystals of the piroxicam : methanol solvate were particularly small and of poor quality and as a result the data is also poor (R_{int} = 23.6%). Anisotropic refinement of the heavy atoms resulted in implausible thermal parameters for a number of atoms and the structure was therefore refined isotropically for the final refinement cycles.

The PX:MeOH solvate crystallises in a 3:1 molar ratio. The crystal structure is again unusual in that piroxicam molecules are again present in mixed tautomeric states, with two zwitterionic molecules and one non-ionised molecule in the asymmetric unit. The symmetry independent PXZ molecules again dimerise in the same way as is seen in form IV, with two moderately strong charge-assisted bifurcated DHAA N^+-H···O hydrogen bonds formed between them (Figure S2.3.1). The MeOH molecule lies below the plane of the dimer and links to one of the PXZ molecules through a further moderately strong, charge assisted O-H···O hydrogen bond (also Figure S2.3.1). Hydrogen bond lengths and angles for these interactions are provided in Table S2.3.1.

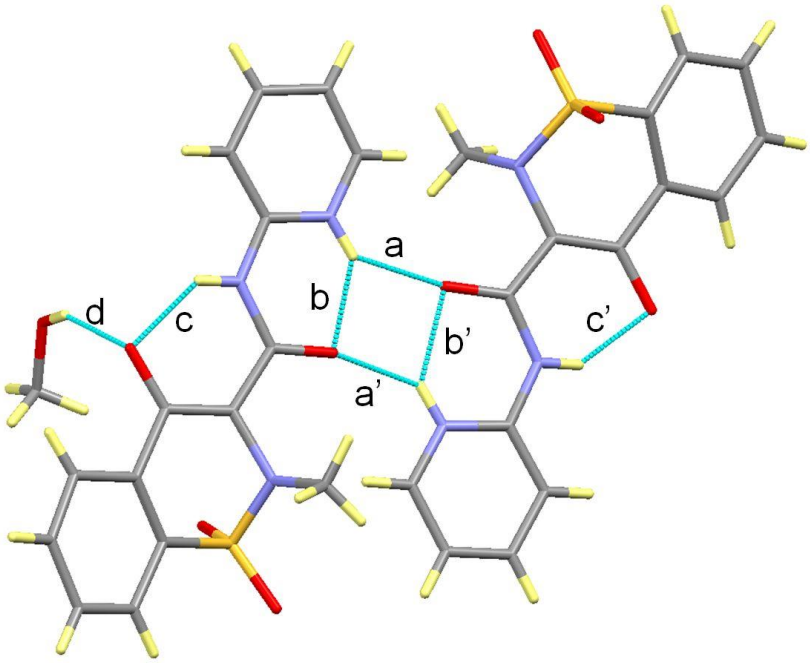

Figure S2.3.1. *The PXZ dimer in the piroxicam: methanol solvate and the methanol molecule hydrogen bonded to the enolate oxygen through an O-H···O hydrogen bond.*

Table S2.3.1. *Hydrogen bond distances and angles in the PXZ dimer in the piroxicam : methanol solvate (refer to Figure S2.3.1 for key). Values with no errors are due to hydrogen atoms being placed on calculated positions. Note: Due to the poor quality data, heavy atoms were refined anisotropically resulting in the poor precision of the D···A values.*

H-Bond	D-H (Å)	H···A (Å)	D···A (Å)	∠D-H···A (°)
a	0.86	2.20	2.86(2)	134
a’	0.86	2.20	2.83(3)	130
b	0.86	1.92	2.58(3)	132
b’	0.86	1.97	2.64(3)	134
c	0.86	1.94	2.64(3)	137
c’	0.86	1.81	2.55(3)	143
d	0.90(7)	2.05(10)	2.88(2)	151(19)

The PXN molecule links PXZ dimers through weak C-H···O hydrogen bonds with the enolate oxygen of both PXZ molecules (pyridine C···O = 3.31(4) Å and benzene C···O = 3.48(3) Å) (Figure S2.3.2). The PXN molecule also links to the MeOH molecule through a moderately strong N-H···O hydrogen bond (N···O = 3.04 (3)Å) with the hydroxyl oxygen acting as acceptor (also Figure S2.3.2). A weak hydrogen bond also occurs between the MeOH methyl C-H and the pyridine nitrogen (C···N = 3.24(4) Å). The PXZ molecules also link to the PXN molecules through C-H···O hydrogen bonds between the benzene ring C-H groups and both the amide oxygen (C···O = 3.38(3) Å) and the sulfonyl oxygen (C···O = 3.22(4) Å) (Figure S2.3.3). The intramolecular hydrogen bond of the PXN molecule is strong with an O···O distance of 2.50(2) Å.

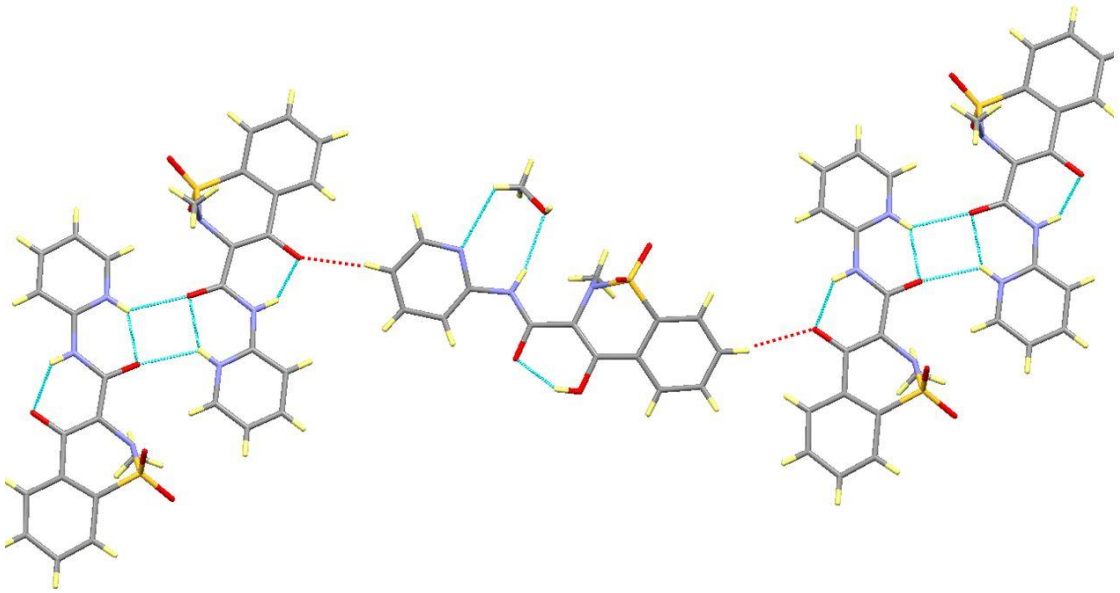

Figure S2.3.2. *The PXN molecule linking PXZ dimers through weak C-H···O hydrogen bonds involving the enolate oxygen atoms (red dashed lines) in the piroxicam : methanol solvate.*

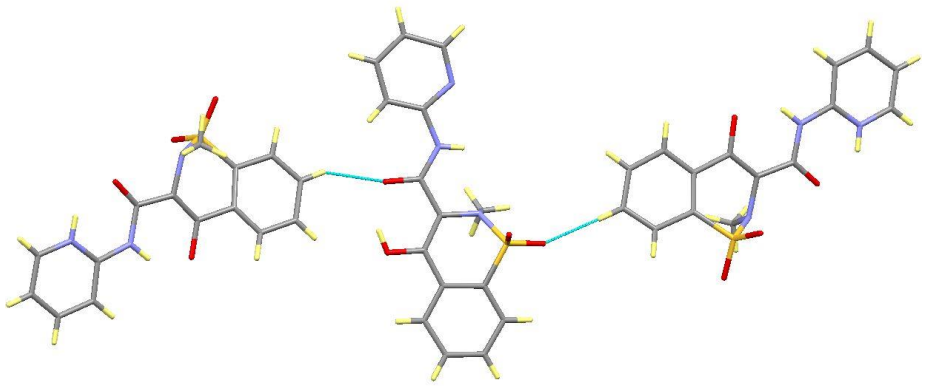

Figure S2.3.3. *Weak C-H···O hydrogen bonds involving the benzene C-H groups of PXZ molecules and the amide and sulfonyl oxygen atoms of the PXN molecules in the piroxicam : methanol solvate.*

The structure is layered (Figure S2.3.4) with the MeOH molecule linking the PXN molecules to PXZ molecules above. Further weak C-H···O hydrogen bonds occur between the PXN molecules with other PXN molecules and PXZ molecules in the layer above involving the sulfonyl oxygen atoms (Figure S2.3.5a). Similar interactions are also present between PXZ molecules - both with adjacent PXZ molecules and PXZ molecules above the plane of the PXZ molecule (Figure 2.3.5b).

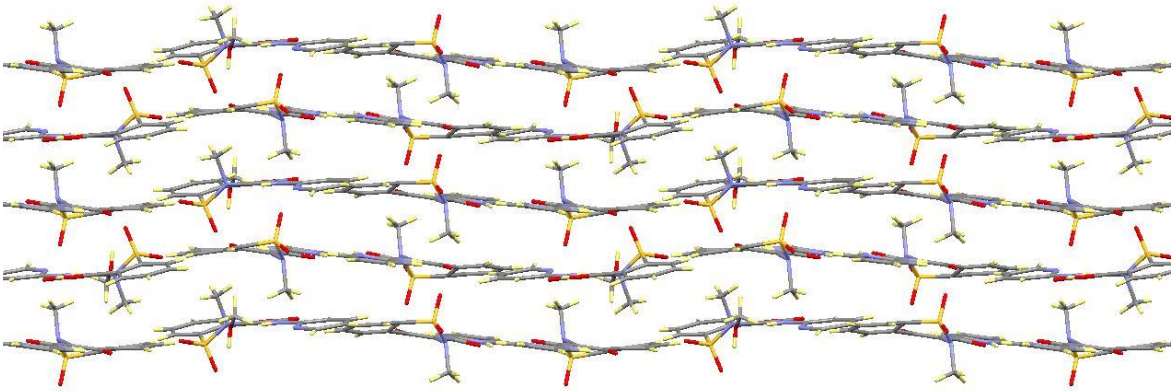

Figure S2.3.4. *Layers in the piroxicam : methanol solvate.*

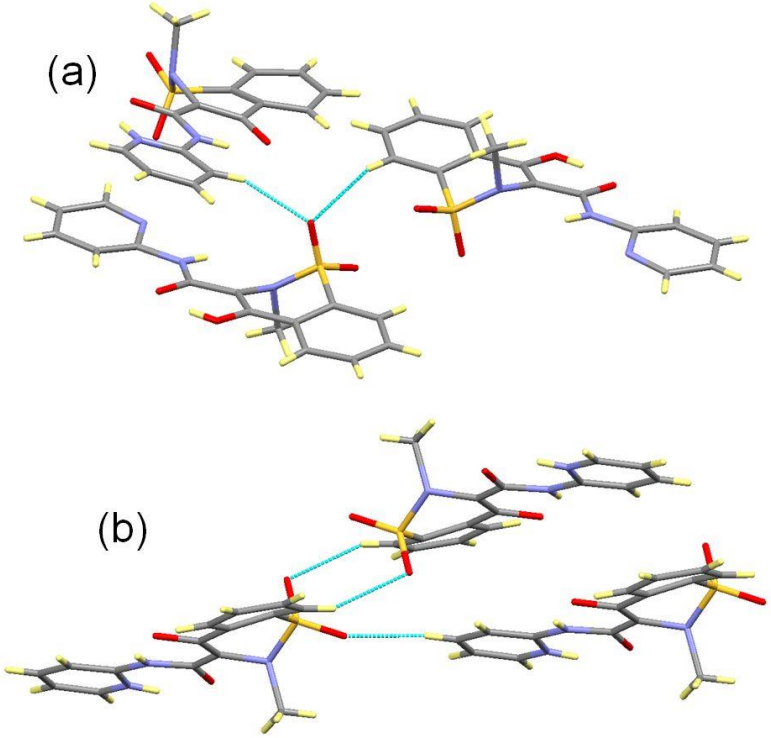

Figure S2.3.5. C-H···O *hydrogen bonds in the piroxicam : methanol solvate involving the sulfonyl oxygen atoms between (a) the PXN molecule and the PXN and PXZ molecules above and (b) PXZ molecules with other PXZ molecules above and adjacent to them.*

Section S3. New Solid Forms of Gallic Acid (4)

S3.1 Porous Gallic Acid Monohydrate (4-H_2O)

Single crystals were grown by solvent evaporation at room temperature using piracetam as the co-molecule and methanol as the solvent. Single crystal X-ray diffraction data for this complex were collected on a Bruker AXS Apex II CCD diffractometer at 100K. The crystals were thin needles and diffracted poorly resulting in weak data.

The water oxygen (O6) has elongated thermal parameters suggesting it may be disordered across two or more positions although this disorder could not be modelled from the available data. The water hydrogen atoms could not be located - likely a result of the disorder of the molecule.

All H-atoms were identified from the Fourier difference synthesis. The positions of the hydrogen atoms were allowed to freely refine but the size of the thermal parameters were constrained to be proportional to the atom to which they were bonded.

An excess of electron density was present in the channels, indicating the presence of disordered solvent molecules. The disordered solvent molecules could not be resolved and the electron density was therefore removed from the final refinement cycle using the SQUEEZE procedure[5] and the number of electrons estimated. The estimate of 120 electrons in the unit cell (in two channels) could correspond to a mixture of water and/or methanol, but a definite conclusion has not been reached due to the small quantities of pure material obtainable; this prevented any other techniques such as TGA being applied. The channels are unlikely to contain piracetam molecules as the electron count per void is lower than that of a piracetam molecule, and also the volume of space per void is smaller than that in which a piracetam molecule could be housed.

The porous gallic acid monohydrate form has a single GA molecule and a single water molecule in the asymmetric unit. The GA molecules dimerise through the typical carboxylic acid dimer formed by moderately strong O-H···O hydrogen bonds (a in Figure S3.1.1). Weaker OH···O hydrogen bonds between the hydroxyl groups (b and c in Figure S3.1.1) link the GA molecules into large rings forming the structural frame of the channels. The oxygen of the water molecule has large, elongated anisotropic displacement parameters (Figure S3.1.2), suggesting it possibly has a large degree of freedom. As a consequence, no water hydrogen atoms could be located (all other hydrogen atoms were located using the difference Fourier synthesis). The hydroxyl O-H of one GA molecule forms a moderately strong O-H···O hydrogen bond to the water oxygen (d in Figure S3.1.1). Although hydrogen atoms were not located, the hydrogen bonding of the water molecule is inferred from the

neighbouring atoms. The water appears to form another moderately strong O-H···O hydrogen bond to the hydroxyl oxygen of another GA molecule (e in Figure S3.1.1). Hydrogen bond distances and angles for these interactions are presented in Table S3.1.1.

Table S3.1.1. *Hydrogen bond distances and angles in the porous gallic acid monohydrate (refer to Figure S3.1 for key). Note: Hydrogen bond e is a proposed hydrogen bond between the GA molecules and the disordered water molecule; water hydrogen atoms could not be located.*

H-Bond	D-H (Å)	H···A (Å)	D···A (Å)	∠D-H···A (°)
a	1.22(4)	1.48(4)	2.619(3)	152(3)
b	0.84(3)	1.97(3)	2.783(3)	164(3)
c	0.98(4)	2.00(3)	2.838(3)	143(3)
d	0.93(4)	1.76(4)	2.668(3)	166(3)
e	-	-	3.008(3)	-

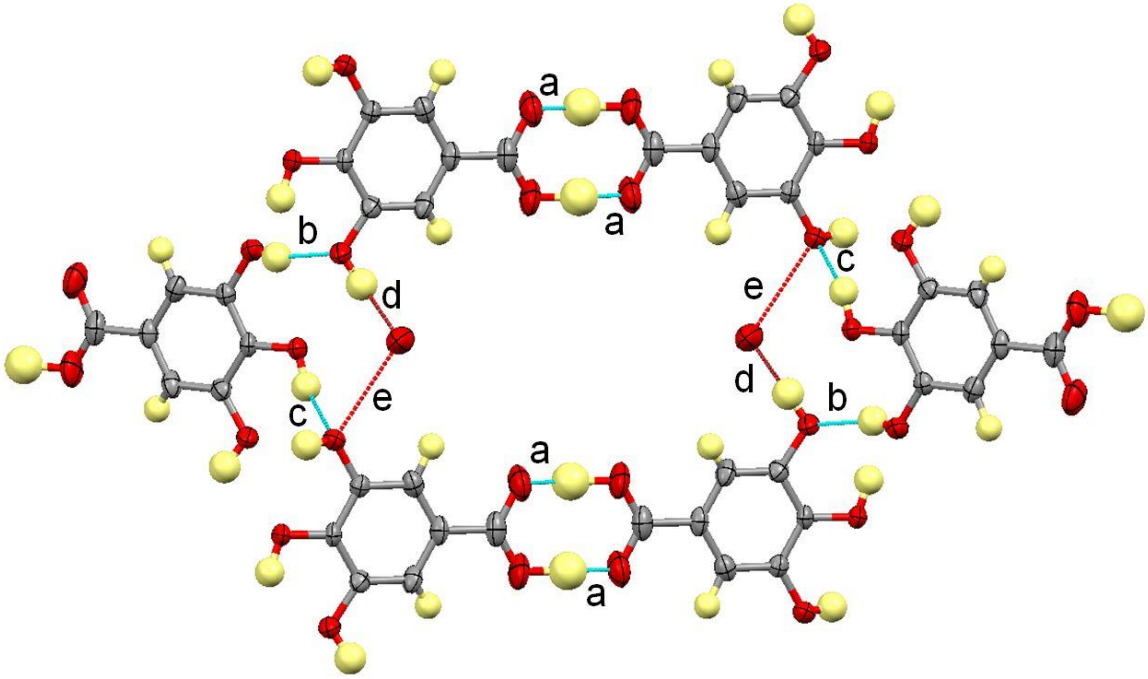

Figure S3.1.1. *Hydrogen bonding forming the pore in the porous gallic acid monohydrate crystal structure.*

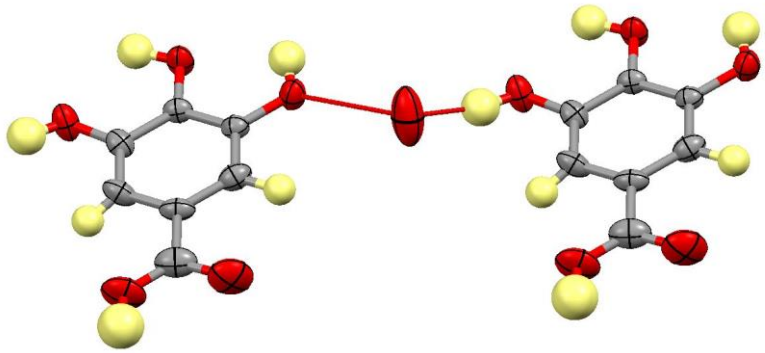

Figure S3.1.2. *The elongated anisotropic displacement parameters of the water oxygen atom relative to the two GA molecules to which it forms hydrogen bonds.*

The hydrogen bonding between the hydroxyl groups (b and c in Figure S3.1.1) links rings parallel to each other to form the channels (Figure S3.1.3), with each GA molecule forming hydrogen bonds to two other GA molecules through these interactions. The channels account for a significant proportion of the unit cell volume (Figure S3.1.4), with approximately 5.0% of the unit cell volume (47.60 $Å^3$) accessible to solvent water molecules (using a probe with a van der Waals radius of 1.4 Å). The channels contain disordered solvent molecules which could not be resolved. The SQUEEZE procedure[6] was therefore used to remove and estimate the electron density from the channel prior to the final refinement cycle. An estimate of 69 electrons per unit cell was given which could be accounted for by roughly ten water molecules or 4 methanol molecules although a definite conclusion could not be reached.

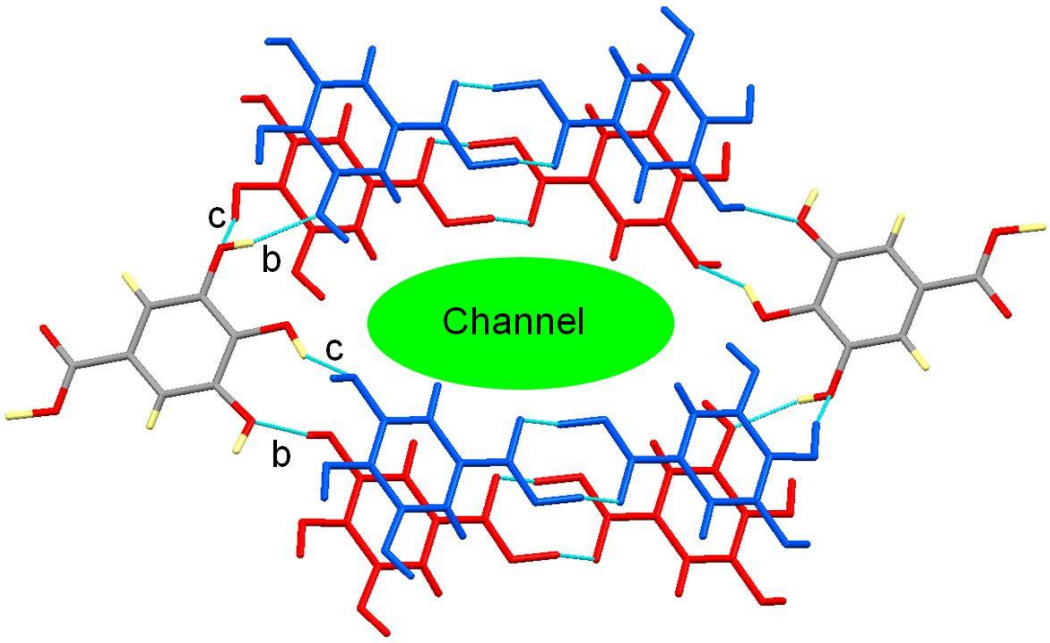

Figure S3.1.3. *Formation of channels in the porous form of gallic acid monohydrate (PGAM). Hydrogen bonding between hydroxyl groups links the large rings parallel to each other to form the channel. The blue GA dimers lie in front of the red dimers, parallel to their plane.*

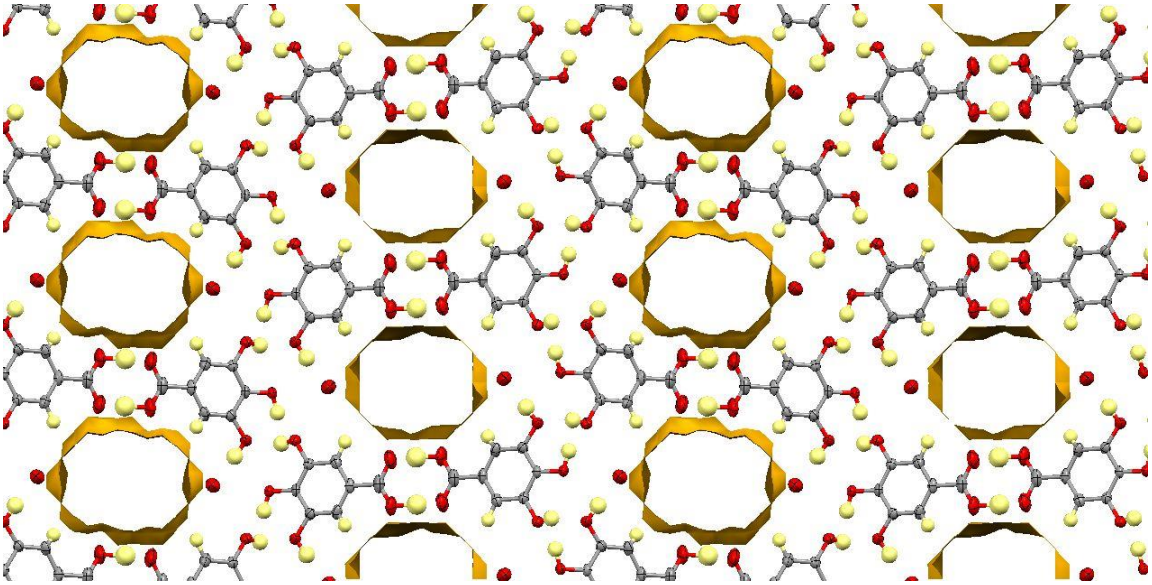

Figure S3.1.4. *Relative arrangement of the channels in the porous gallic acid monohydrate.*

S3.2. Piracetam Gallic Acid Molecular Complex (3-4)

Single crystals were grown by solvent evaporation at room temperature using ethyl acetate as the solvent. Single crystal X-ray diffraction data for this complex were collected on a Rigaku R-AXIS RAPID Image Plate diffractometer at 100K.

The PTM:GA complex contains one molecule of each component in the asymmetric unit. The PTM and GA molecules dimerise, although the dimer is not of the amide-carboxylic acid type as might have been expected. Instead, the dimer is formed through the amide group forming hydrogen bonds with the neighbouring hydroxyl groups in the 3- and 4-positions, with one OH group acting as a hydrogen bond donor to the amide carbonyl and the oxygen of the other as an acceptor for the amide N-H group. This forms a hydrogen bonded $R^2_2(9)$ ring (a and b in Figure S3.2.1). Both hydrogen bonds in the dimer are moderately strong (see Table S3.2.1). The second amide N-H also forms a moderately strong N-H···O hydrogen bond with the GA hydroxyl in the 5-position (c in Figure S3.2.1). This hydroxyl group also forms an O-H···O hydrogen bond to the carboxylic acid carbonyl of another GA molecule (e in Figure S3.2.1). The GA molecules form two moderately strong O-H···O hydrogen bonds to the pyrrolidone carbonyl of PTM through the hydroxyl in the 3-position and the carboxylic acid hydroxyl (d and f in Figure S3.2.1).

Molecules in the structure are stacked in two directions (Figure S3.2.2a), with weak interactions holding the stacks together (Figure S3.2.2b). The molecules are stacked in pairs of PTM

molecules followed by pairs of GA molecules. PTM molecules in the stacks are linked by weak C-H···O hydrogen bonds between the C-H groups in the pyrrolidone rings and the amide oxygen atoms (C···O = 3.224(4) Å). An acetamide C-H group of PTM forms C-H···π interactions with the aromatic ring of GA (approx. 3.345 Å between the carbon and the plane of the ring). The aromatic rings of GA molecules are then stacked upon each other via π···π interactions (approx. 3.386 Å between the plane of the rings).

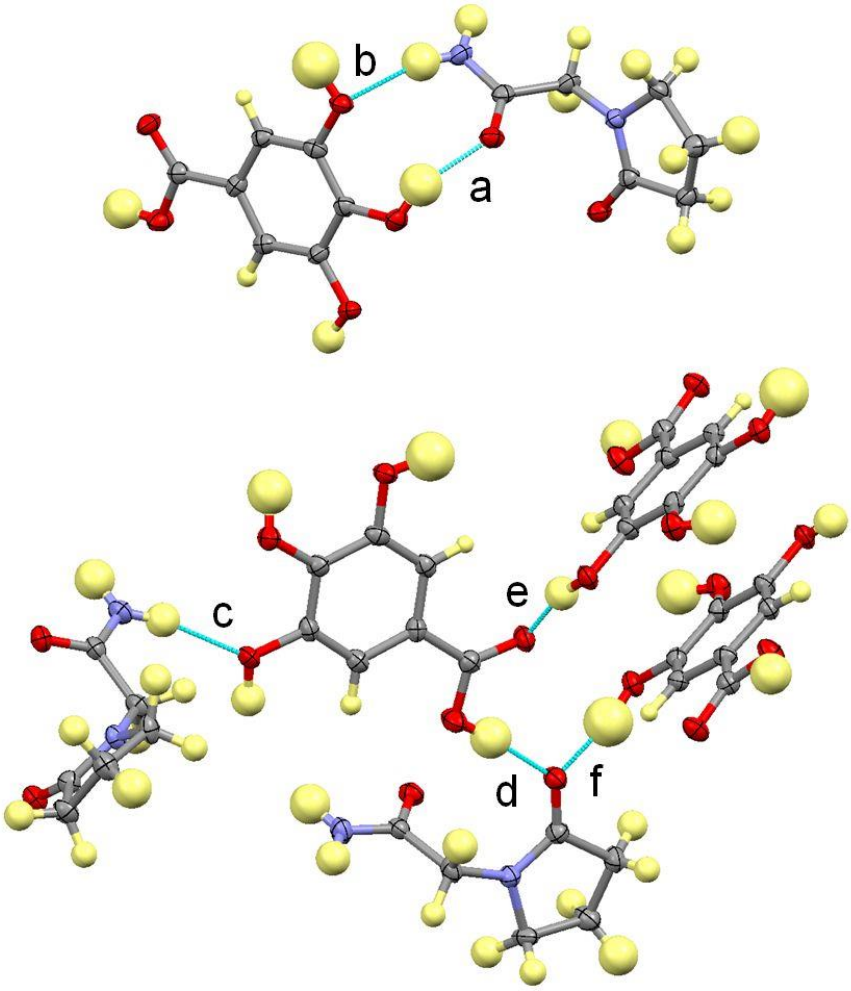

Figure S3.2.1. *The heterodimer formed by PTM and GA molecules in the PTM:GA complex (top) and the remaining NH···O and OH···O hydrogen bonds that occur between PTM and GA molecules (bottom).*

Table S3.2.1. *Hydrogen bond lengths and angles in the piracetam : gallic acid complex (refer to Figure S3.2.1 for key).*

Complex	H-Bond	D-H (Å)	H···A (Å)	D···A (Å)	∠D-H···A (°)
PTM:GA	A	0.95(5)	1.84(5)	2.726(4)	156(5)
	b	0.91(5)	2.07(5)	2.954(4)	164(4)
	c	0.96(4)	2.01(4)	2.950(4)	167(4)
	d	0.94(5)	1.72(5)	2.662(3)	173(3)
	e	0.99(4)	1.73(4)	2.707(3)	167(3)
	f	0.99(5)	1.69(5)	2.675(3)	170(5)

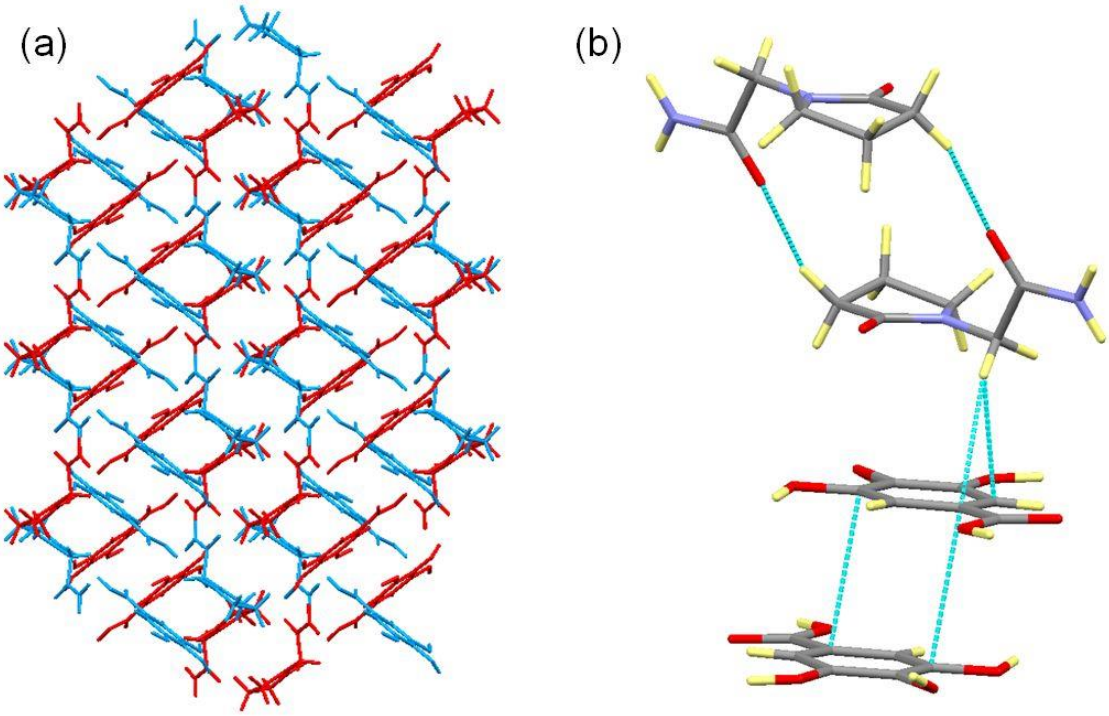

Figure S3.2.2. *Crystal packing in the PTM:GA complex. (a) The molecules arranged in stacks running in two directions (the different parallel stacks are coloured red and blue); (b) the interactions between stacked molecules.*

S4. Crystallographic Data for the New Solid Forms

	PX III (1-III)	**PX IV (1-IV)**	**PX : MeOH (1-MeOH)**	**PGAM (4.H_2O)**	**PTM:GA (3-4)**
Formula	C15 H13 N3 O4 S1	C15 H13 N3 O4 S1	3(C15 H13 N3 O4 S1), (C1 H4 O1)	(C7 H6 O5), (H2O)	(C6 H10 N2 O2), (C7 H6 O5)
M/g mol^{-1}	331.35	331.35	1026.09	188.13	312.28
T/K	100	100	100	100	100
Space Group	P-1	P-1	P-1	$P2_1/n$	$P2_1/c$
a/Å	7.8557(3)	12.6899(9)	7.037(2)	3.6803(3)	12.554(2)
b/Å	10.1043(4)	14.6928(9)	12.917(4)	27.724(2)	8.8499(15)
c/Å	10.4713(5)	20.5097(16)	25.467(8)	9.3579(7)	12.6253(17)
α	80.602(2)	84.866(2)	84.077(7)	90	90
β	68.952(2)	74.669(3)	89.174(7)	94.397(3)	103.988(5)
γ	69.742(2)	84.683(2)	83.327(6)	90	90
V/$Å^3$	727.01(5)	3663.7(4)	2287.0(12)	952.00(12)	1361.1(4)
Z	2	10	2	4	4
ρ_{cal}/ g cm^{-3}	1.514	1.502	1.443	1.299	1.524
μ/mm^{-1}	0.248	0.246	0.236	0.117	0.125
θ Range/°	2.09 - 30.52	3.04 - 24.71	3.02 - 20.82	1.47 - 28.09	3.08 - 27.48
Ref (meas. / ind.)	16541 / 4375	40126 / 11817	14992 / 4731	12141 / 2115	10236 / 3044
Observed>2σ	3102	6294	2059	929	1684
Rint	0.0746	0.1060	0.2357	0.0676	0.0958
Completeness %	98.6	94.7	99.4	91.8	97.5
Parameters	260	1039	292	136	263
GooF	0.968	1.011	1.440	0.907	1.056
R_1 (obs)	0.0407	0.0803	0.2271	0.0568	0.0562
R_1 (all)	0.0678	0.1562	0.3371	0.1327	0.1209
wR2 (all)	0.1011	0.2812	0.5325	0.1636	0.1633
$\rho_{max,min}$/e $Å^{-3}$	0.536, -0.468	1.161, -0.790	1.498, -1.383	0.323, -0.205	0.355, -0.427

References

1. F. Vrecer, M. Vrbinc, A. Meden, *Int. J. Pharm.* 256, p3-15 (2003).
2. B. Kojic-Prodic, Z. Ruzic-Toros *Acta Cryst.* **B38** (11), p2948-2951 (1982).
3. S. L. Childs, K. I. Hardcastle, *Cryst. Growth Des.* **7** (7), p1291-1304 (2007).
4. J. Bordner, J. A. Richards, P Weeks, E. B. Whipple, *Acta Cryst.* **C40**, p989-990 (1984).
5. A.L.Spek, *Acta Cryst*. **D65**, 148-155 (2009).